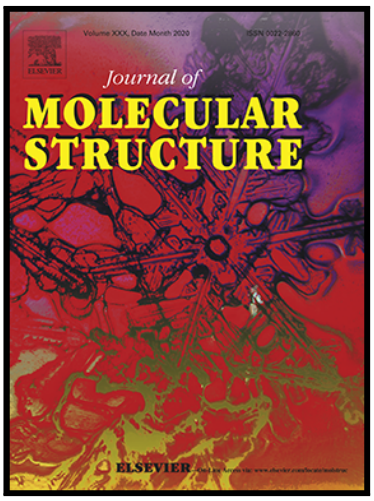

Synthesis, crystal structure, Hirshfeld surface analysis, biological evaluation, DFT calculations, and in silico ADME analysis of 4-arylidene pyrazolone derivatives as promising antibacterial agents

Imene Sehout , Houssem Boulebd , Raouf Boulcina , Sara Nemouchi , Lamia Bendjeddou , Amina Bramki , Hocine Merazig , Abdelmadjid Debache

PII: S0022-2860(20)31900-1
DOI: https://doi.org/10.1016/j.molstruc.2020.129586
Reference: MOLSTR 129586

To appear in: *Journal of Molecular Structure*

Received date: 20 September 2020
Revised date: 21 October 2020
Accepted date: 3 November 2020

Please cite this article as: Imene Sehout , Houssem Boulebd , Raouf Boulcina , Sara Nemouchi , Lamia Bendjeddou , Amina Bramki , Hocine Merazig , Abdelmadjid Debache , Synthesis, crystal structure, Hirshfeld surface analysis, biological evaluation, DFT calculations, and in silico ADME analysis of 4-arylidene pyrazolone derivatives as promising antibacterial agents, *Journal of Molecular Structure* (2020), doi: https://doi.org/10.1016/j.molstruc.2020.129586

Highlights

- An ultrasound-assisted synthesis of a series of pyrazolone derivatives has been described.
- Single crystal X-Ray diffraction analysis of compound **3i** has been reported.
- Theoretical calculations using DFT/B3LYP method have been performed.
- The antibacterial activity of all the synthesized compounds was evaluated.
- *In silico* ADME parameters have been studied.

Synthesis, crystal structure, Hirshfeld surface analysis, biological evaluation, DFT calculations, and *in silico* ADME analysis of 4-arylidene pyrazolone derivatives as promising antibacterial agents

Imene Sehout[1], Houssem Boulebd[1,*], Raouf Boulcina[1], Sara Nemouchi[1], Lamia Bendjeddou[2], Amina Bramki[3], Hocine Merazig[2], Abdelmadjid Debache[1,*]

[1]*Laboratory of Synthesis of Molecules with Biological Interest, University of Frères Mentouri Constantine 1, Constantine, Algeria.*
[2]*Unité de Recherche Chimie de l'Environnement et Moléculaire Structurale, Université Frères Mentouri Constantine 1, 25000, Constantine, Algeria*
[3]*Laboratory of Mycology, Biotechnology and Microbial Activity, Mentouri Constantine 1 University, 25000 Constantine, Algeria.*
** Corresponding authors: boulebd.houssem@umc.edu.dz (H. Boulebd); a_debache@yahoo.fr (A. Debache)*

Abstract

The present paper describes an ultrasound-assisted synthesis of a series of 4-arylidene-1*H*-pyrazol-5(4*H*)-one derivatives (**3a-i**) catalyzed by sulfamic acid. The prepared compounds were characterized by physical and spectroscopic techniques and for compound **3i** by single crystal X-ray diffraction analysis. Theoretical calculations such as molecular structure optimization, frontier molecular orbitals, molecular electrostatic potential, and molecular descriptors have been performed in order to get insight into the molecular structure and chemical reactivity of the synthesized compounds. The antibacterial activity of all compounds was assessed against six bacterial strains, and it was found that these compounds are good inhibitors of Gram-positive bacteria rather than Gram-negative. In addition, good oral bioavailability was predicted for all compounds by *in silico* calculations of ADME (absorption, distribution, metabolism, and elimination) and pharmacokinetic parameters.

Keywords: Pyrazolone; crystal structure; DFT calculations; antibacterial activity; ADME parameters.

1. Introduction

Heterocycles constitute the basic skeleton for a large variety of compounds with chemical, biological, pharmacological, and industrial interests [1]. Consequently, heterocyclic chemistry became the center of interest of a great community of experimental chemists and theorists. Also, a large number of biologically active natural substances are heterocyclic compounds [2, 3]. Among them, pyrazole is an integral part in several biologically active natural products, in particular alkaloids [4]. These derivatives attracted much attention in recent years, because of their numerous applications as pharmaceutical agents, photographic couplers, chelating agents in coordination chemistry, and agrochemical products [5-8].

Pyrazolones are a very important class of the pyrazole family, they are known since more than one century [9]. This scaffold is present in a number of commercial drugs. For example (Figure 1), phenazone is a pyrazolone derivative with analgesic and anti-inflammatory properties [10]. Metamizole is a pyrazolone derivative that acts as an antipyretic and has modest analgesic and spasmolytic properties [11]. Propyphenazone has anti-inflammatory, analgesic, and antipyretic activities [12]. Also, benzpiperylone is used as an anti-inflammatory agent [13]. Other pyrazolone derivatives have been reported to exhibit several biological activities such as antioxidant [14], antitumor [15], anti-tuberculosis [16], anti-cancer [17], anti-inflammatory [18], and antimicrobial [19-21]. Their analogues were also employed as fluorescent herbicide [22], dyes and pigments [23], chelating agents [24], and polymers [25]. The various applications of these compounds aroused a great interest on behalf of chemists by searching for new biologically active molecules and by the development of new methods leading to this kind of compounds. In this context, ultrasonic organic synthesis is considered as green approach towards organic synthesis as it offers simple, clean, fast, efficient and economic technique for organic synthesis [26, 27].

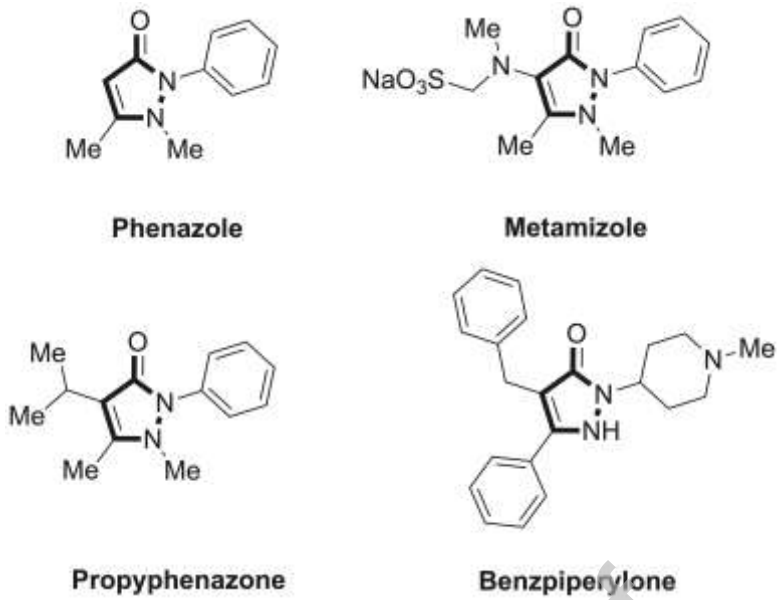

Figure 1. Some commercialized drugs based on pyrazolone scaffold.

As part of an ongoing program in search of new methods of organic synthesis [28-31], as well as the development of new biologically active compounds [31, 32], we present in this paper a simple, rapid, and high yielding ultrasonic synthesis of a series of 4-arylidene pyrazolone derivatives **3a-i**. Molecular structures of these compounds were fully characterized by various physical and spectroscopic techniques, and also, in the case of compound **3i**, by X-ray crystal structure analysis. Theoretical calculations based on DFT/B3LYP method were performed in order to get insight into the molecular structure and chemical reactivity of compound **3i** as representative molecule. Antibacterial activity of the synthesized compounds was evaluated against six bacterial strains; *Staphylococcus aureus*, *Bacillus subtilis*, *Escherichia coli*, *Pseudomonas aeruginosa*, *Enterococcus faecalis*, and *Klebsiella pneumoniae*. Finally, *in silico* ADME calculations were carried out in order to investigate the pharmacokinetic profile of the prepared compounds.

2. Experimental section

2.1. Materials and instrumentation

All reagents as well as the solvents were acquired from Sigma Aldrich and employed without further purification. ^{1}H NMR and ^{13}C NMR spectra were determined using Brucker 250 and 400 MHz spectrometers. *J* values are in hertz (Hz). Chemical shifts are expressed in parts per million downfield from internal standard TMS. Ultrasonication was performed in a Bandelin SONOREX Digital 10 P ultrasonic bath with a frequency of 35 kHz (Built-in heating, 30−80 °C thermostatically adjustable). The reaction flask was located at the maximum energy area in the cleaner, and the surface of the reactants was placed slightly lower than the level of the water. Observation of the surface of the reaction solution during vertical adjustment of vessel depth will show the optimum position by the point at which maximum surface disturbance occurs. Crystal suitable for single crystal X-ray diffraction was selected using a polarizing microscope. The crystal was coated with Paratone oil and mounted on a loop for data collection and the lattice parameters were determined using a Bruker APEX II CCD diffractometer (SADABS; Sheldrick, 2002).

2.2. Synthesis

4-Arylidene pyrazolone derivatives were prepared as follows: to a mixture of aldehyde derivatives and 3-methyl-1-phenyl-pyrazol-5-one in the proportions (1:1) molar in the presence of 5 mL of ethanol, was added a catalytic amount of sulfamic acid (10 mol %). The reaction was carried out under ultrasonic irradiation (100 %: 35 kHz) at 35 °C. The reaction is monitored by TLC using ethyl acetate/hexane as eluent. After completion, the reaction mixture was allowed to cool to room temperature. Then 5 mL of petroleum ether was added. The precipitate formed is recovered by filtration and recrystallized from ethanol to give pure products in good to excellent yields.

(E)-4-(2,3,4-Trimethoxybenzylidene)-3-methyl-1-phenyl-1H-pyrazol-5(4H)-one **(3a)**: Yellow crystals, yield 61%, M.p = 213-215 ºC.^{1}H NMR (250 MHz, DMSO-d_6): δ 7.60 (d, J = 8.1 Hz, 2H, Ar-H), 7.30 (s, 1H, H-CSp^2), 7.25 (d, J = 8.2 Hz, 2H, Ar-H), 7.03-7.09 (m, 1H, Ar-H), 6.50 (d, J = 8.5 Hz, 1H, H-Ar), 6.15 (d, J = 8.4 Hz, 1H, Ar-H), 3.68 (s, 9H, OCH_3), 2.34 (s , 3H, CH_3).^{13}C NMR (62.5 MHz, DMSO-d_6): δ 164.3 (CO), 149.1 (C-Ar), 148.8 (^{3}C), 147.3 (Csp^2), 142.6 (C-Ar), 139.0 (C-Ar), 136.7 (C-Ar), 128.0 (^{4}C), 126.6 (C-Ar), 124.8 (C-Ar), 122.1 (C-Ar), 119.4 (C-Ar), 108.2 (C-Ar), 107.2 (C-Ar), 50.1 (OCH_3), 13.6 (CH_3).

(E)-4-(2,4-Dimethylbenzylidene)-3-methyl-1-phenyl-1H-pyrazol-5(4H)-one **(3b)**: Yellow crystals, yield 61%, M.p =193-195 ºC. ^{1}H NMR (400 MHz, DMSO-d_6): δ 8.66 (d, J = 12 Hz, 1H, Ar-H), 7.94-7.99 (m, 2H, Ar-H), 7.30 (s, 1H, H-Sp2), 7.41 (t, J = 12 Hz, 2H, Ar-H), 7.10-7.13 (m, 1H, Ar-H), 6.85 (d, J = 8.0 Hz, 2H, Ar-H), 3.13 (s, 6H, 2CH_3), 2.30 (s, 3H, CH_3). ^{13}C NMR (100 MHz, DMSO-d_6): δ 162.9 (CO), 154.3 (^{3}C), 152.0 (Csp^2), 148.6 (C-Ar), 139.4 (C-Ar), 137.9 (C-Ar), 129.2 (^{4}C), 124.4 (C-Ar), 121.7 (C-Ar), 119.5 (C-Ar), 118.6 (C-Ar), 111.8 (C-Ar), 40.4 ($^4CH_3$), 39.8 (CH_3), 13.7 ($^2CH_3$).

(E)-4-(3-Hydroxy-4-methoxybenzylidene)-3-methyl-1-phenyl-1H-pyrazol-5(4H)-one **(3c)**: Yellow crystals, yield 85%, M.p =224-226 ºC. ^{1}H NMR (400 MHz, DMSO-d_6): δ 8.46 (m, 1H, Ar-H), 8.03 (dd, J^3 =12.0 Hz , J^4 =4.0 Hz, 1H, Ar-H), 7.93 (d, J =8.0 Hz, 2H, Ar-H), 7.65 (s, 1H, H-CSp^2), 7.43 (t, J =12 Hz, 2H, Ar-H), 7.18 (t, J = 8.0 Hz, 1H, Ar-H), 7.12 (d, J = 12.0 Hz, 1H, Ar-H), 3.91 (s, 3H, CH_3), 2.32 (s, 3H, CH_3). ^{13}C NMR (100 MHz, DMSO-d_6): δ 162.2 (CO), 153.4 (C-Ar), 152.2 (^{3}C), 149.2 (Csp^2), 146.5 (C-Ar), 138.8 (C-Ar), 129.7 (C-Ar), 129.2 (^{4}C), 126.9 (C-Ar), 124.8 (C-Ar), 123.8 (C-Ar), 120.4 (C-Ar), 118.7 (C-Ar), 112.0 (C-Ar), 56.2 (OCH_3), 13.6 (CH_3).

(E)-3-Methyl-1-phenyl-4-(thiophen-2-ylmethylene)-1H-pyrazol-5(4H)-one **(3d)**: Yellow crystals, yield 75%, M.p = 121-123 ºC. ^{1}H NMR (250 MHz, DMSO-d_6): δ 7.64 (d , J = 8.7 Hz, 1H, Ar-H), 7.60 (d, J = 8.5 Hz, 1H, Ar-H), 7.32 (s, 1H, H-CSp^2), 7.30 (d, J = 8.1Hz, 2H,

Ar-H), 7.25-7.29 (m, 1H, H-Ar), 7.14-7.19 (m, 1H, Ar-H), 6.90 (d, *J*=8.5 Hz, 2H, Ar-H), 2.31 (s, 3H, CH_3). ^{13}C NMR (62.5 MHz, DMSO-d_6): δ 164.1 (CO), 146.8 (^3C), 140.2 (Csp^2), 137.5 (C-Ar), 137.2 (^4C), 130.1 (C-Ar), 129.9 (C-Ar), 129.0 (C-Ar), 128.5 (C-Ar), 126.8 (C-Ar), 124.1 (C-Ar), 120.8 (C-Ar), 13.4 (CH_3).

(E)-4-(4-methoxybenzylidene)-3-methyl-1-phenyl-1H-pyrazol-5(4H)-one **(3e)**: Yellow crystals, yield 75%, M.p = 135-137 ºC. ^1H NMR (250 MHz, DMSO-d_6): δ 8.54 (d, *J* = 8.9 Hz, 2H, Ar-H), 7.89 (d, *J* = 8.2 Hz, 2H, Ar-H), 7.34 (s, 1H, H-CSp^2), 7.32 (d, *J* = 8.1Hz , 2H, Ar-H), 7.10 (t , *J* = 14.8 Hz, 1H, Ar-H), 6.94 (d, *J* = 8.8 Hz, 2H, Ar-H), 3.84 (s, 3H, OCH_3), 2.24 (s, 3H, CH_3). ^{13}C NMR (62.5 MHz, DMSO-d_6): δ 163.2 (CO), 161.6 (C-Ar), 150.6 (^3C), 146.5 (Csp^2), 138.0 (C-Ar), 136.2 (C-Ar), 128.1 (^4C), 125.7 (C-Ar), 124.0 (C-Ar), 119.3 (C-Ar), 118.3 (C-Ar), 113.6 (C-Ar), 55.0 (OCH_3), 12.8 (CH_3).

(Z)-4-((1H-indol-2-yl)methylene)-3-methyl-1-phenyl-1H-pyrazol-5(4H)-one **(3f)**: Yellow crystals, yield 78%, M.p = 241-243 ºC. ^1H NMR (400 MHz, DMSO-d_6): δ 12.06 (s, 1H, NH), 9.86 (s, 1H, H-Ind), 8.00-7.97 (m, 2H, Ar-H), 7.90-7.82 (m, 2H, Ar-H), 7.25 (s, 1H, H-CSp^2), 7.48-7.23 (m, 4H, Ar-H), 7.14-7.08 (m, 1H, Ar-H), 2.36 (s, 3H, CH_3). ^{13}C NMR (100 MHz, DMSO-d_6): δ 162.8 (CO), 150.5 (^3C), 138.6 (C-Ar), 138.2 (C-Ar), 136.3 (^4C), 135.9 (C-Ar), 132.9 (C-Ar), 128.2 (Csp^2), 128.0 (C-Ar), 123.7 (C-Ar), 123.5 (C-Ar), 121.8 (C-Ar), 118.4 (C-Ar), 117.2 (C-Ar), 112.4 (C-Ar), 112.1 (C-Ar), 12.7(CH_3).

(E)-4-(4-hydroxybenzylidene)-3-methyl-1-phenyl-1H-pyrazol-5(4H)-one **(3g)**: Yellow crystals, yield 82%, M.p = 231-233 ºC. ^1H NMR (250 MHz, DMSO-d_6): δ 10.45 (s, 1H, OH), 8.48 (d, *J* = 8.7 Hz, 2H, Ar-H), 7.88 (d , *J* = 8.6 Hz, 2H, Ar-H), 7.37 (s, 1H, H-CSp^2), 7.31 (d, *J* = 8.3 Hz, 2H, Ar-H), 7.12-7.06 (m, 1H, Ar-H), 6.87 (d, *J* = 8.7 Hz, 2H, Ar-H), 2.27 (s, 3H, CH_3). ^{13}C NMR (62.5 MHz, DMSO-d_6): δ 162.8 (CO), 161.8 (C-Ar), 150.9 (^3C), 147.5 (Csp^2), 136.9 (C-Ar), 128.2 (^4C), 124.0 (C-Ar), 122.8 (C-Ar), 119.6 (C-Ar), 115.6 (C-Ar), 12.9 (CH_3).

(E)-4-(4-(dimethylamino)benzylidene)-3-methyl-1-phenyl-1H-pyrazol-5(4H)-one **(3h)**: Yellow crystals, yield 84%, M.p = 191-193 ºC. ^{1}H NMR (250 MHz, DMSO-d_6) : δ 8.57-8.53 (m, 2H, H-Ar), 7.91 (d, *J* = 7.8 Hz , 2H, Ar-H), 7.28-7.34 (m, 2H, Ar-H), 7.26 (s, 1H, H-Sp^2), 7.07 (t , *J* = 7.4 Hz, 1H, Ar-H), 6.67 (d, 2H, Ar-H), 3.09 (s, 6H, 2CH_3), 2.26 (s, 3H, CH_3). ^{13}C NMR (62.5 MHz, DMSO-d_6): *δ* 162.2 (CO), 153.2 (C-Ar), 150.8 (^{3}C), 147.2 (Csp^2), 138.5 (C-Ar), 136.9 (C-Ar), 128.1 (^{4}C), 123.6 (C-Ar), 121.0 (C-Ar), 119.7 (C-Ar), 118.3 (C-Ar), 110.7 (C-Ar), 39.5 (N(CH_3)$_2$), 12.9 (CH_3).

(E)-4-(3,5-dimethoxybenzylidene)-3-methyl-1-phenyl-1H-pyrazol-5(4H)-one (**3i**): Red crystals, Yield 87%, M.p = 133-135 ºC. ^{1}H NMR (400 MHz, DMSO-d_6) : *δ* 7.87-7.93 (m, 3H, H_{arom}), 7.41-7.48 (m , 2H, Ar-H), 7.73 (s, 1H, H-$C_{ethylenic}$), 7.17-7.23 (m, 2H, Ar-H), 6.76-6.75 (m, 1H, Ar-H), 3.82 (s, 6H, OCH_3), 2.31 (s, 3H, CH_3). ^{13}C NMR (100 MHz, DMSO-d_6): δ 161.8 (CO), 160.7 (C-Ar), 160.6 (C-Ar), 152.2 (^{3}C), 148.9 (Csp^2), 138.5 (C-Ar), 135.0 (C-Ar), 129.4 (C-Ar), 127.4 (C-Ar), 125.1 (^{4}C), 118.9 (C-Ar), 118.3 (C-Ar), 111.8 (C-Ar), 109.0 (C-Ar), 106.3 (C-Ar), 55.9 (OCH_3), 13.5 (CH_3).

2.3. Crystal structure analysis

X-ray diffraction data were acquired at 293 K on a Bruker APEX II CCD diffractometer employing graphite crystal monochromatized MoKα radiation source (0.71073A). Data collection, indexing with reduction and absorption corrections were carried out using APEX2, SAINT and SADABS programs, respectively. The structure was solved using direct methods (SIR92) [33] and refined by full-matrix least-squares techniques on F2 with SHELXL-2014 [34] operating within WinGX [35]. All H atoms were positioned geometrically and refined as riding atoms, with C-H = 0.93 and 0.96 aromatic and methyl respectively; and constrained to ride on their parent atoms, with U iso (H) = 1.2U eq. General crystallographic details for the **3i** are provided in Table 1. The figures were made using the Mercury program [36]. CCDC number 2012606 contains the supplementary crystallographic data for this paper. These data

can be obtained free of charge from The Cambridge Crystallographic Data Centre via http://www.ccdc.cam.ac.uk/data_request/cif.

Table 1. Single-crystal X-ray data and structure refinement details for **3**i.

Compound	**3i**
Formula	$C_{19}H_{18}N_2O_3$
M r	322.35
Temperature/K	296
Wavelength/Å	0.71073
Crystal system	Triclinic
Space group, N°	$P\bar{1}$, 2
a/Å	7.4058(7)
b/Å	10.0747(8)
c/Å	11.644(1)
α/ °	71.265(4)
β/ °	78.205(5)
γ / °	83.181(4)
V/Å^3	804.05(12)
Z	2
μ(mm^{-1})	0.09
D_c (g cm Å^{-3})	1.331
Diffractometer	Bruker APEX-II CCD
Absorption correction	-
No. of measured, independent and observed [$I > 2\sigma(I)$] reflections	14493/4015/2991
R_{int}	0.047
Data/restraints/parameters	4015/0/217
R_1 /wR_2 [I > 2σ(I)]	0.059 / 0.203
Goodness-of-fit on F^2	1.07
$\Delta\rho_{max}$, $\Delta\rho_{min}$ (e Å^{-3})	0.27 / - 0.19

2.4. Computational details

Density functional theory (DFT) calculations have been carried out using Gaussian09 software [37]. The B3LYP functional [38, 39] and the 6-311G(d,p) basis set have been used for all calculations [40, 41]. All of the ground states were confirmed by vibrational frequency analysis (no imaginary frequency). Electronegativity, chemical softness, chemical hardness, and electrophilic index were calculated from HOMO/LUMO energies method as reported in our previous studies [42-45].

2.5. Antibacterial activity evaluation

2.5.1. Preparation of microorganism tests

Microbial support is composed of six bacterial strains: four ATCC strains (American Type Culture Collection), which are: *Staphylococcus aureus* (ATCC 25923), *Bacillus subtilis* (ATCC 6633), *Escherichia coli* (ATCC, 25922), *Pseudomonas aeruginosa* (ATCC, 27853), and two clinical strains namely *Enterococcus faecalis* and *Klebsiella pneumoniae.* Antibacterial tests were performed from young cultures (18 to 24 h), in the exponential growth phase. The opacity of the bacterial suspensions in sterile physiological water was equivalent to 0.5 McFarland (a bacterial concentration estimated at 10^6 CFU/mL) [46].

2.5.2. Discs technique

To evaluate the antibacterial activity of the prepared compounds, they were dissolved in dimethylsulfoxide (DMSO) in order to obtain a concentration of 10 mg/mL. Then, sterile discs of 6 mm diameter were prepared from Whatman paper No. 1, containing 10 µL of the products. After drying, the discs were carefully placed on Petri dishes containing Mueller-Hinton medium previously seeded by the tested bacteria. Before incubation at 37°C, the dishes were left for 2h at 4°C to allow the diffusion of the bioactive substances [47, 48]. Results' reading was done after 18 to 24 h. The antibacterial activity was evaluated by measuring the zone of growth inhibition of bacteria surrounding the wells. Ciprofloxacin

served as the positive control. DMSO was taken as the negative control which did not produce any significant zone of inhibition. Any extending of inhibition zone around discs, even a small diameter, was considered as a positive result. It should be noted that three repetitions were performed, and the diameters of the inhibition zones were measured in millimeter.

3. Results and discussion

3.1. Synthesis

In order to optimize the reaction conditions, the condensation of 3-methyl-1-phenyl-5-pyrazolone with 4-hydroxybenzaldehyde was chosen as a reaction model. Initial study on Knoevenagel condensation was tested in EtOH at room temperature in the presence of sulfamic acid (10 mol%) as catalyst, but the reaction rate decreased and did not complete even after 3 h (Table 2, entry 1). The same reaction was then conducted at reflux (Table 2, entry 2) then at 35 ºC under ultrasound irradiations (Table 2, entry 3). According to the obtained results, the reaction works better with ultrasonic irradiations.

In the next step, a number of solvents such as EtOH, EtOH/H_2O, THF, and ethyl acetate were also tested while fixing the catalytic amount of sulfamic acid (10 mol%), the temperature at 35 ºC, and the ultra-sound frequency (Table 2, entries 4-6). It was found that the use of ethanol as a solvent dramatically reduces the reaction time with improved product yield.

After that, we evaluated the required amount of the catalyst for this condensation. In the presence of 5 mol% of the catalyst, the reaction proceeded efficiently after 4.5 h (Table 2, entry 7). By further increasing the catalyst amount, no appreciable improvement in the product yield and reaction time was observed (Table 2, entries 8 and 9).

To determine the appropriate temperature of this condensation, we investigated the model reaction using 10 mol% of the catalyst at different temperatures: 25, 45, and 65 ºC

(Table 2, entries 10-12), however, the product yield diminished to 34, 10, and 51% respectively, indicating that a 35 ºC was adequate for optimal results considering the reaction time and product yield (Table 2, entry 3).

In continuation of this method, to further improve the yield and decrease the reaction time, the effect of various amplitude of ultrasonic irradiation on the reaction was studied (Table 2, entries 13-15). As shown in Table 2, the best result was found with an amplitude of 100% with 83% isolated yield after 0.5 h (Table 2, entry 3). Therefore, the optimal conditions for the synthesis of pyrazolone derivatives are the use of 10 mol% of sulfamic acid in ethanol at 35°C under ultrasonic irradiation (100% of amplitude).

Table 2. Optimization of the operating conditions for the synthesis of arylidene pyrazolone **3g** (equimolar reaction of 3-methyl-5-phenyl-pyrazol-5-one and 4-hydroxybenzaldehydes in the presence of sulfamic acid as catalyst).

Entry	Solvent	Cat. (mol %)	T (°C)	Ultrasound amplitude (%)	Time (h)	Yield (%)*
1	EtOH	10	Ref lux	-	3	80
2	EtOH	10	R.T	-	3	49
3	EtOH	10	35	100	0.5	83
4	THF	10	35	100	2	87
5	Aqueous EtOH	10	35	100	6	51
6	Ethyl acetate	10	35	100	6	59
7	EtOH	5	35	100	4.5	82
8	EtOH	20	35	100	5	30
9	EtOH	30	35	100	6	73
10	EtOH	10	25	100	2	34
11	EtOH	10	45	100	1	10
12	EtOH	10	65	100	1	51

13	EtOH	10	35	80	0.75	52
14	EtOH	10	35	50	0.5	72
15	EtOH	10	35	30	0.5	32

* Yield of the isolated product

Using the optimized reaction conditions, a series of pyrazolone derivatives was synthesized as shown in Table 3. As can be seen from Table 3, the reaction was found to be general and applicable to the aromatic aldehydes bearing various substituents such as nitro, chloro, methyl, methoxyl, hydroxyl, and N,N-dimethylamino, etc. Furthermore, in the case of heteroaromatic aldehydes such as 2-thiophenecarboxaldehyde (compound **3d**) and 3-indolcarboxaldehyde (compound **3f**), the reactions also could proceed smoothly under the reaction conditions led to the formation of the corresponding compounds in good yields. The experimental results show that both aromatic aldehydes bearing electron-withdrawing or electron-donating groups reacted easily to afford the desired products in high yields. The proposed molecular structures of the synthesized compounds were confirmed by ^{1}H NMR and ^{13}C NMR, spectroscopy techniques and, for compound **3i**, by single crystal X-ray diffraction analysis.

Table 3. Sulfamic acid–catalyzed synthesis of arylidene pyrazolones **3a-i** under ultrasonic irradiation.

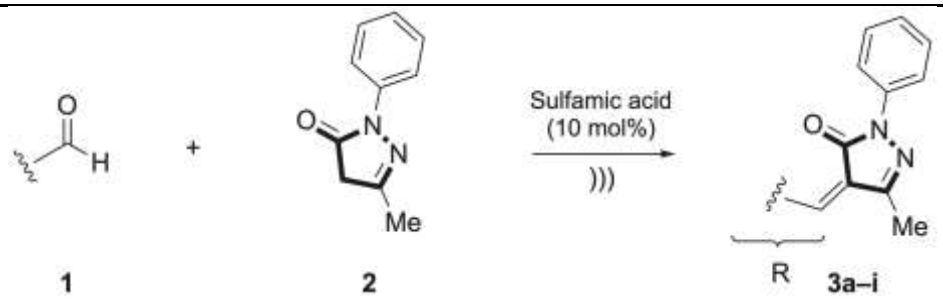

1 **2** **3a–i**

Compound	R	Times (min)	T_{fus}(°C)	Yields (%)
3a	3,4,5-$(OCH_3)_3$-C_6H_2	60	213-215	61
3b	2,4-$(CH_3)_2$-C_6H_3	180	193-195	61
3c	3-OH-4-CH_3-C_6H_3	45	224-226	85
3d	Thiophen-2-yl	130	121-122	75
3e	4-OCH_3-C_6H_4	40	135-137	75
3f	1*H*-indol-2-yl	90	241-243	78
3g	4-OH-C_6H_4	30	231-233	83
3h	4-$N(CH_3)_2$-C_6H_4	150	191-193	84
3i	3,5-$(OCH_3)_2$-C_6H_3	120	133-135	87

We propose a plausible mechanism for the formation of the synthesized pyrazolones (Scheme 2). In the first step, sulfamic acid plays two roles: that of protonating the aldehyde function, which thus promotes the nucleophilic attack on the electropositive center of the carbonyl, while the second is the removal of hydrogen from the active methylene of pyrazolone. The hydroxypyrazolone intermediate which is rapidly formed gives rise to the formation of the desired products after dehydration.

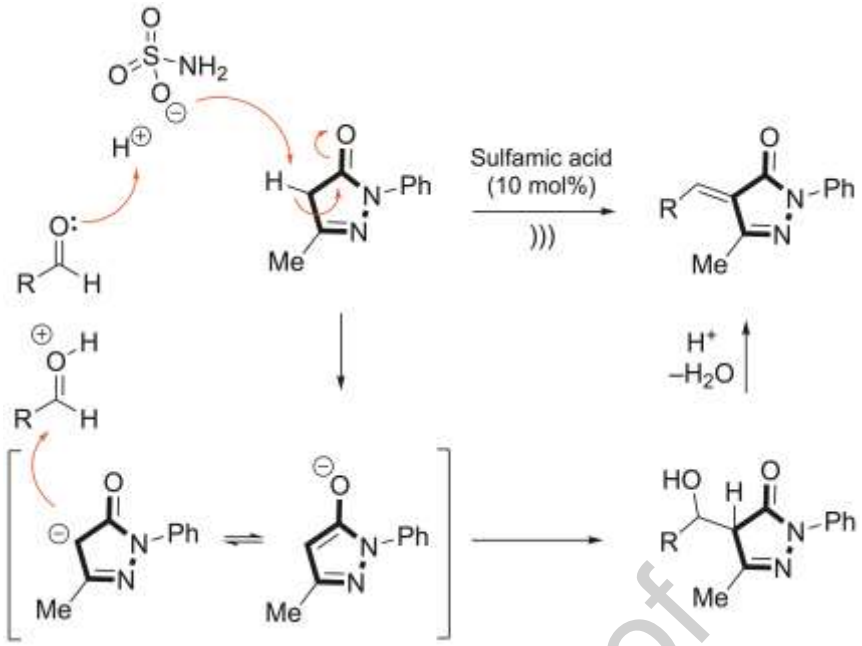

Scheme 2. Proposed mechanism for the synthesis of pyrazolone derivatives **3a-i**.

3.2. Crystal structure

Single-crystal structure analysis shows that compound **3i** crystallizes in the triclinic space group $P\bar{1}$, with one symmetry-independent molecule in the asymmetric unit (Figure 2). All bond lengths and angles in this compound have regular values [49]. For example, the C7—O1 bond length of 1.2148(1) Å is in good agreement with that for a C=O double bond. The C9-N2 bond length of 1.2906 (1) Å is consistent with that for a normal C=N double bond, which indicates that the compound exists in the keto form. The phenyl, benzene and pyrazolone rings systems are essentially planar with maximum deviations from the mean plane of 0.0011, 0.0117, 0.0025 respectively. The mean plane of the phenyl ring system subtends a dihedral angle of 5.20 (7)Å with the pyrazolone ring, which is close to the value of 6.2 (2) and 7.58 (12) Å reported for a related compound, 4-isopropylidene-3-methyl-1-(3-nitrophenyl)-1H-pyrazol-5(4H)-one and 1-(3-Methyl-5-oxo-1-phenyl-1,5-dihydro-4H-pyrazol-4-ylidene) propyl] benzene sulfonohydrazide respectively which also exist in the keto form [50, 51];

while the dihedral angle between the benzene ring system and the pyrazolone ring system is 3.38(8) Å.

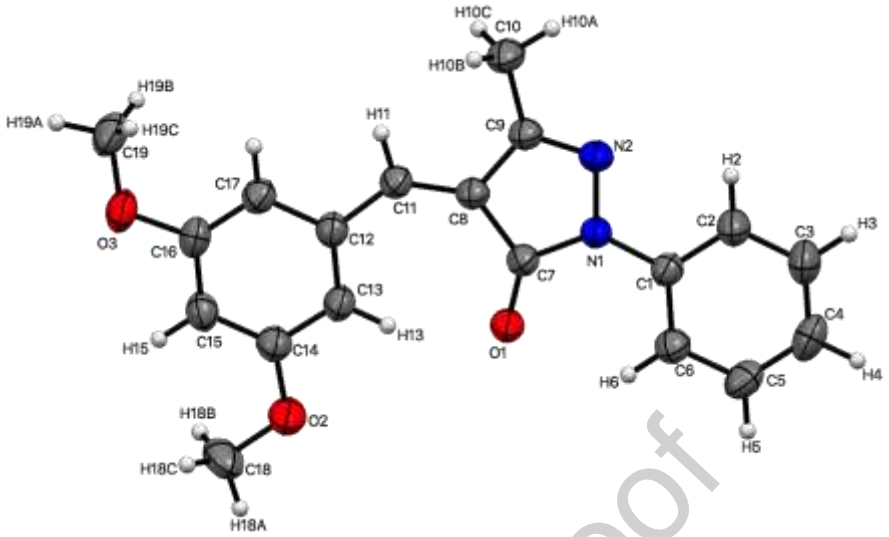

Figure 2. ORTEP view of the asymmetric unit of title compound, showing the atom numbering scheme. Displacement ellipsoids are drawn at the 50% probability level.

The structure of title compound contains two distinct intramolecular hydrogen bonds between the oxo group of pyrazolone and the carbon atoms from phenyl and benzene respectively. These interactions are observed between C6-H6…O1 and C13-H13…O1 (Figure 3, Table. 4). The crystal structure of compound **3i** can be described as a three-dimensional network, the molecules are interconnected to inversion dimers of the $R^2_2(10)$ motif [52]; by C5-H5…O1^{i} (i: –x+1, -y, -z+1) intermolecular hydrogen bonds. These dimers are interconnected into three-dimensional structure via C-H…π hydrogen bonds, connecting one of the methyl group of methoxy fragment and the centroid of phenyl ring, with a distance of 2.79 Å and an angle of 143°. The three-dimensional structure is also stabilized by two π…π interactions involving two centroids of pyrazolone and benzene rings [ring centroid separation *Cg*1⋯ *Cg*3^{i} = 3.7238(4) Å and *Cg*1⋯ *Cg*3^{ii}= 3.7960(4) Å, where *Cg*1 and *Cg*3 are the centroid of the N1-N2-C9-C8-C7 and C12-C17 ring, respectively; symmetry codes: *(i)* x,1-y,1-z; *(ii)* 1-x,1-y,1-z] (Figure 4).

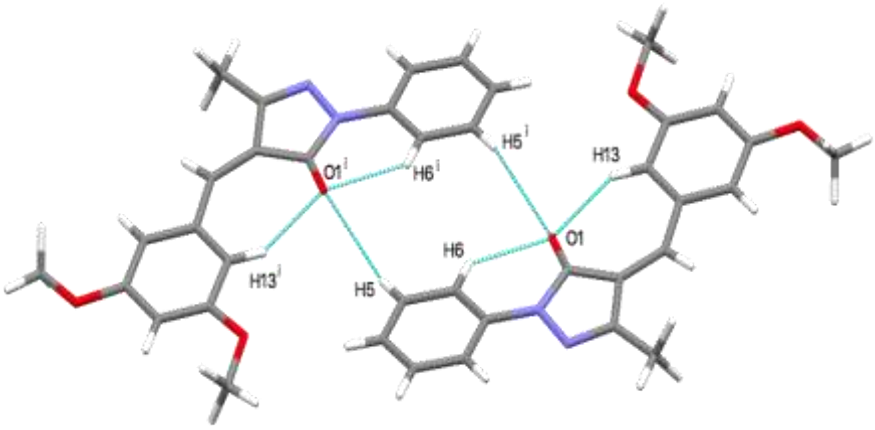

Figure 3. Intra and inter molecular hydrogen bonds in compound **3i**.

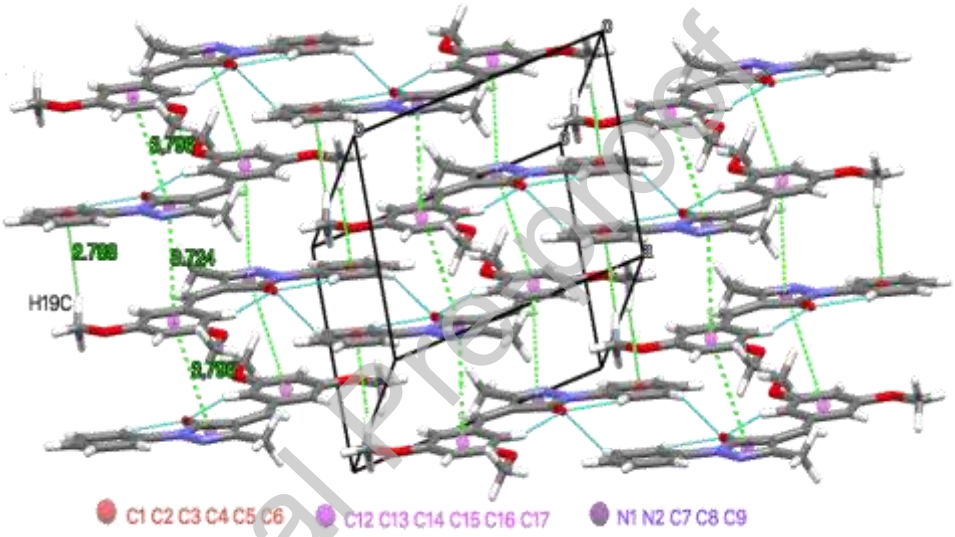

Figure 4. A view of the three-dimensional network of the compound **3i**, showing the C- H···π hydrogen bonds and π… π interactions.

Table 4. Hydrogen-bond geometry (Å, °). *Cg*2 is the centroid of the C1–C6 ring.

D-H…A	D-H	H…A	D…A	D-H…A
C5-H5…O1^{i}	0.9300	2.5800	3.4317(3)	152.00
C6-H6…O1	0.9300	2.2900	2.9094(3)	124.00
C13H13…O1	0.9300	2.1500	2.9882(3)	149.00
C19-H19C…*Cg*2^{ii}	0.9300	2.7900	3.5997(3)	60.000

Symmetry codes : (i) –x+1, -y, -z+1; (ii) –x, -y+1, -z+1

3.3. Hirshfeld surface analysis

Hirshfeld surface mapped over d_{norm}, and its related two-dimensional fingerprints have been computed in order to quantify the intermolecular contacts of the crystal structure of compound **3i** using Crystal Explorer 17.5 software [53]. The obtained results are shown in Figures 5 and 6. As can be seen from the 3D Hirshfeld surface represented in Figure 5, two intermolecular hydrogen bonds between O1 and H5 are present for compound **3i** with distances shorter than Van der waals (Vdw) radii (red spots on the Hirshfeld surface). It was revealed also the presence of two H…H bonds, H10–H4 and H2–H2 with distances nearly equal to the sum of Vdw radii (white areas on the Hirshfeld surface). The 2D fingerprint plots depicted in Figure 6 show the contribution of the different types of intermolecular interactions. It was found that the H…H interaction has the highest interatomic contact contributions (53.0%), followed by C…H (16.2%), and O…H (13.4%) interactions.

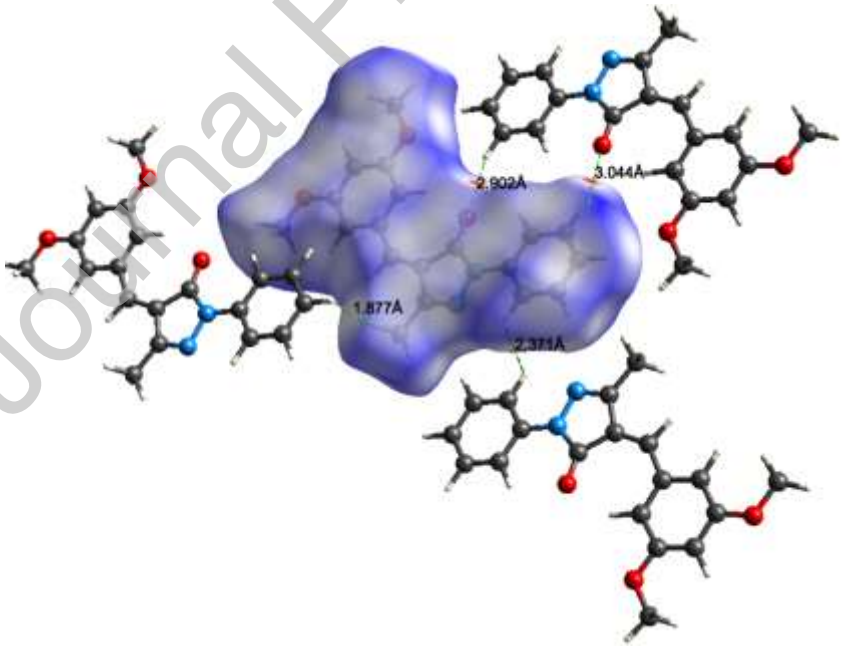

Figure 5. The three-dimensional Hirshfeld surface of compound **3i** mapped over d_{norm} in the range –0.1121 to 1.2526 a. u.

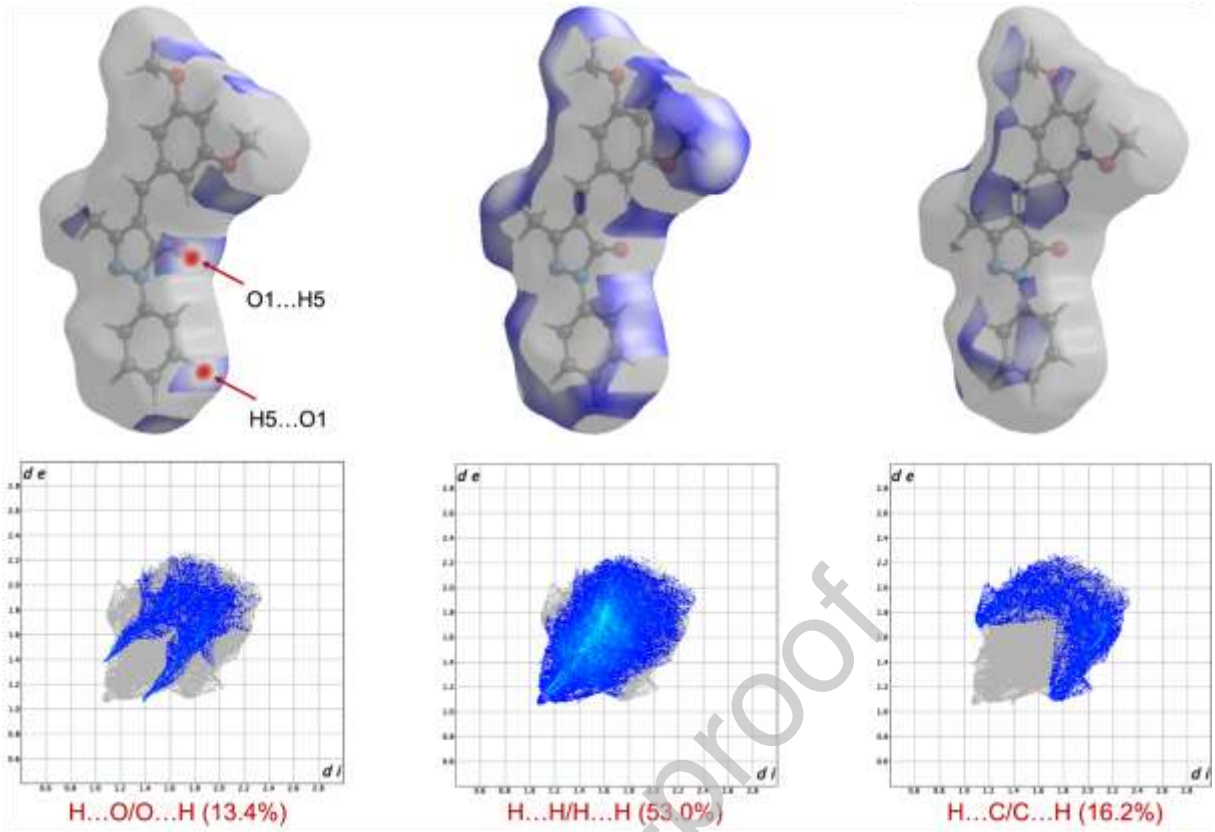

Figure 6. Two-dimensional fingerprints of compound **3i** resolved into H…O/O…H, H…H/H…H, and H…C/C…H contacts (blue areas).

3.4. Theoretical investigations

DFT calculations at B3LYP/6-311G(d,p) level of theory have been carried out in order to gain more insights into the molecular structure and chemical reactivity of compound **3i** as an example molecule. Firstly, the molecular geometry of compound **3i** has been optimized and the most stable structure was compared with that obtained from the crystal structure analysis. Figure 7 shows the DFT-optimized molecular structure of compound **3i**, and Table S1 represents some selected experimental and theoretical geometry parameters. As shown, good correlations are observed between the experimental and theoretical structures. The bond lengths and angles have nearly the same values, while the dihedral angles are slightly deviated by 3.40° to 3.47°. This result confirms the accuracy of B3LYP/6-311G(d,p) method for geometry optimization. In this geometry, compound **3i** adopts a planar structure due to

conjugation of π-electrons over the whole structure of the molecule, which is an indication of its stability.

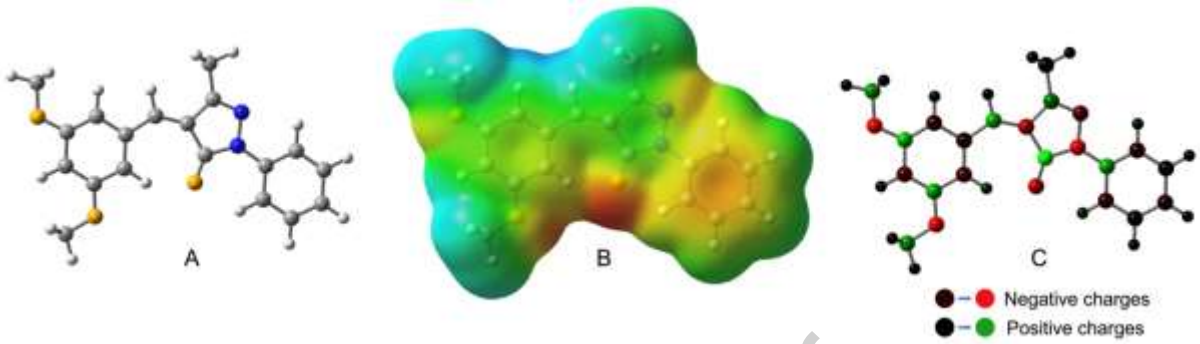

Figure 7. Molecular geometry (A), molecular electrostatic potential (B), and atomic polar tensor charges (C) of compound **3i** obtained in the gas-phase at B3LYP/6-311G(d,p) level of theory.

Using the optimized molecular geometry of compound **3i**, we have calculated at the same level of theory some molecular properties such as frontier molecular orbitals (FMO), atomic charge distributions, and molecular electrostatic potential mapping. FMO are important properties that characterize the chemical reactivity of organic compounds [41, 54, 55]. LUMO (lowest unoccupied molecular orbital) is the easiest orbital to accept electrons and determines the sites for electrophilic attacks, while HOMO is the easiest orbital to donate electrons and determines the sites for nucleophilic attacks. The calculated FMO energies and distributions of compound **3i** are shown in Figure 8. As can be seen, the HOMO is distributed mainly on the pyrazolone and the N-phenyl moieties, whereas the LUMO is located on the pyrazolone, C8-C11 double bond, and the substituted phenyl. These results clearly enlighten the transfer of electron density from the non-substituted phenyl to substituted phenyl moieties. The calculated gap energies (3.05 eV) indicates the high kinetic stability and low chemical reactivity of compound **3i** [56, 57].

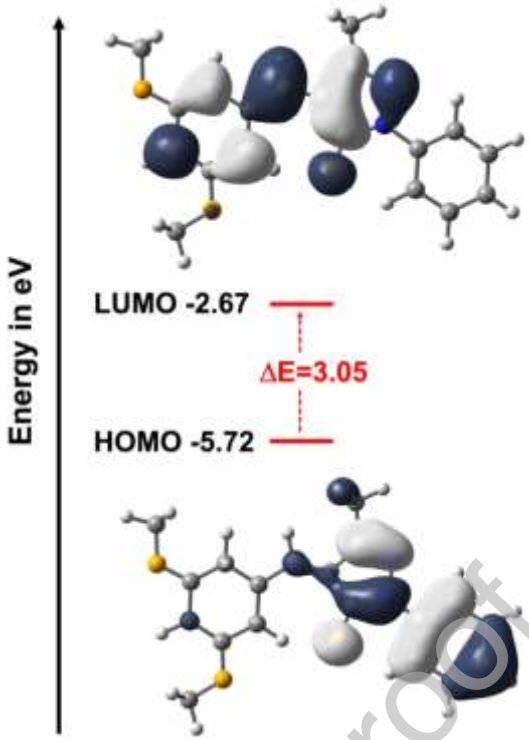

Figure 8. Frontier molecular orbitals of compound **3i** obtained in the gas-phase at B3LYP/6-311G(d,p) level of theory.

The distribution of electrons (charges distribution) in organic compounds is a crucial property, because it determines several physicochemical properties such as solubility, stability, dipole moment, electrostatic potential, vibrational spectroscopy, chemical reactivity, and others [58-60]. The distribution of electrons of compound **3i** has been characterized by computing molecular electrostatic potential (ESP) and the atomic polar tensor charges (APT). The obtained results are presented in Figure 7 and tabulated in Table S2 in supporting information. ESP revealed that the highest positive regions are around the H11 and H17, suggesting that these regions must be the most favorable sites for the attack of nucleophiles. With the APT charges, the highest positive atoms were found to be C9, C12, and C15 with partial charges of 1.05, 0.63, and 0.62, respectively. On the other hand, the highest negative charges are found around the oxygens O1 and O2 with both ESP and APT (-0.94 and -0.69,

respectively). This indicates that these atoms should be the most nucleophilic sites of compound **3i**.

Electronegativity (χ), chemical hardness (η), chemical softness (S), and electrophilic index (ω) are also useful quantitative properties of organic compounds that could be used to predict the chemical stability and reactivity [61-63]. Electronegativity characterizes the capacity of a molecule to attract electrons. The chemical hardness (η) and softness (S) measure the resistance to charge transfer. The electrophilic index is defined as a measure of energy lowering associated with a maximum amount of electron flow between a donor and an acceptor [61-63]. Using HOMO/LUMO energy method, we have calculated all of the mentioned parameters for compound **3i**, and the obtained values are reported in Table S3. From the obtained data, it was found that compound **3i** has a relatively high η value (2.31 and 2.39 eV) and low S value (0.33 eV), indicating high kinetic stability and low chemical reactivity. It presents also high values of χ and ω which reflects that this compound prefers to act as electron acceptor rather than electron donor [42].

3.5. Antibacterial activity

The antibacterial activity of the synthesized pyrazolones **3a-i** was evaluated against six bacterial strains, four ATCC strains namely: *Staphylococcus aureus* (ATCC 25923), *Bacillus subtilis* (ATCC 6633), *Escherichia coli* (ATCC, 25922), *Pseudomonas aeruginosa* (ATCC, 27853), and two clinical strains namely: *Enterococcus faecalis* and *Klebsiella pneumoniae*. Ciprofloxacin was used as the reference drug. The obtained results are shown in Table 5. The results showed that the majority of the products have shown an antibacterial activity against the test bacteria; *S. aureus*, *B subtilis*, and *E. faecalis*, where the averages of the inhibition zones diameters went from 7.0 to 12.5 mm. Furthermore, no inhibition zone was observed with the three tested strains *E. coli*, *P. aeruginosa*, and *K. pneumoniae* (Table 5). Overall, the

most considerable effects are observed with compounds **3a**, **3c**, **3d**, and **3i** which have shown an activity against the three sensitive strains, comparable to the reference drug Ciprofloxacin with a zone of inhibition of 18 mm, followed by compounds **3g** and **3h** against two strains only. However, the two compounds **3b** and **3f** make the exception and they could not inhibit the development of any bacteria. Gram-positive bacteria appear to be more sensitive to the synthesized pyrazolones in comparison with Gram-negative ones. Against Gam-positive bacteria (*S. aureus* and *E. faecalis*), compound **3i** showed the best antibacterial activity with a zone of inhibition of 12.5 mm and 11 mm, respectively. Compound **3d** showed also the best activity among the other derivatives with a zone of inhibition of 11mm against Gam-positive bacteria *B. subtilis*. These results can be explained by the fact that these two groups of microorganisms differ morphologically, because Gram negative bacteria have an outer membrane which is a polysaccharide membrane carrying the lipopolysaccharide structural components [64, 65]. This makes the cell wall impermeable to lipophilic compounds, unlike Gram-positive bacteria, which will be more sensitive because they only have an outer peptidoglycan layer, which is not an effective permeability barrier [64]. As can be concluded from the obtained results, the pyrazolone derivatives **3a-i** are promising antibacterial agents, in particular against Gram-positive bacteria. This result is close to the study reported by P. Khloya et *al*. on the *in vitro* antibacterial activity of pyrazolone derivatives[66].

Table 5. Demonstration of the antibacterial activity of the synthesized pyrazolone derivatives **3a-i** by disks technic.

Compound	*Diameter of zone of inhibition in mm*					
	S. aureus	*B. subtilis*	*E. faecalis*	*E. coli*	*P. aeruginosa*	*K. pneumoniae*
3a	11.0± 1.4	10.5±0.7	8.5±0.7	-	-	-
3b	-	-	-	-	-	-
3c	9.5±0.7	10.0±0.0	9.0±0.0	-	-	-
3d	7.0±0.0	11.0±2.8	9.0±0.0	-	-	-
3e	11.0±0.0	9.5±0.7	10.0±0.0	-	-	-
3f	-	-	-	-	-	-
3g	8.0±0.0	9.5±0.7	-	-	-	-
3h	-	10.0±0.0	7.0±0.0	-	-	-
3i	12.5±0.7	10.5±0.7	11.0±0.0	-	-	-
Ciprofloxacine	18±0.1	18±0.3	18±0.2	16±0.2	20±0.3	22±0.3

(-) : Diameter of the inhibition zone <6 mm

3.6. *In silico* ADME analysis

ADME (absorption, distribution, metabolism and excretion) properties of the synthesized pyrazolones **3a-i** have been estimated using Molinspiration software. Based on Lipinski's rule [67], molecules with good ADME properties should have no more than one violation of the following criteria: number of hydrogen bond donors (n-OHNH) < 5, number of hydrogen bond acceptors (n-ON) < 10, molecular weight < 500 daltons, an octanol-water partition coefficient (milogP) < 5. As indicated in Table 6, all of the studied compounds showed no violation of the mentioned criteria. Thus, these compounds perfectly respect the Lipinski rule. In addition, the calculated percentage of absorption of compounds **3a-i** (80.43–96.65%) suggests that these compounds should be easily absorbed by the human body [68]. These

results indicate that the synthesized pyrazolones **3a-i** have good ADME properties and could be considered as drug candidates.

Table 6. ADME properties of compounds **3a-i.**

Comp.	miLogP	TPSA (^{o}A)	MW	nON	nOHNH	n-rotb	MV	vio.	%Abs
	<5		<500	<10	<5			<1	
3a	2.48	62.60	352.39	6	0	5	320.25	0	86.84
3b	3.00	50.69	301.35	4	1	2	272.59	0	91.06
3c	2.75	34.90	268.34	3	0	0	234.33	0	96.65
3d	3.68	34.90	290.37	3	0	2	276.74	0	96.65
3e	2.91	44.13	292.34	4	0	3	269.16	0	93.38
3f	3.68	34.90	290.37	3	0	2	276.74	0	96.65
3g	2.38	55.12	278.31	4	1	2	251.63	0	89.49
3h	2.96	38.13	303.38	4	0	3	289.52	0	95.50
3i	2.90	53.37	322.36	5	0	0	294.71	0	90.11

Logarithm of partition coefficient between n-octanol and water (miLogP); Topological polar surface area (TPSA); Molecular weight (MW); Number of hydrogen bond acceptors (n-ON); Number of hydrogen bond donors (n-OHNH); Number of rotatable bonds (n-rotb); Molecular volume (MV); Lipinski's violation (vio.); Percentage of absorption (%Abs).

4. Conclusion

A green and efficient ultrasound-assisted synthesis of a series of 4-arylidene-1H-pyrazol-5(4H)-one derivatives (**3a-i**) has been reported. All the compounds were fully characterized by spectroscopy techniques and for compound **3i** by single crystal X-ray diffraction analysis. Molecular geometry, electronic properties, and physicochemical descriptors have been investigated using DFT calculations in order to understand the chemical reactivity and

stability of the studied pyrazolones. The study of the antibacterial activity was revealed that the synthesized compounds are promising inhibitors of tested Gam-positive bacterial strains *S. aureus*, *B. subtilis*, and *E. faecalis*. However, none of the compounds were found to be as effective as the standard drug Ciprofloxacin. The results revealed also that the synthesized compounds are not effective against the tested Gam-negative bacterial strains *E. coli*, *P. aeruginosa*, and *K. pneumonia*. This result is in line with reported studies on pyrazolone derivatives. In addition, *in silico* ADME calculations suggested that these compounds have a good pharmacokinetic profile.

Acknowledgements

We would like to thank MESRS (Ministère de l'Enseignement Supérieur et de la Recherche Scientifique, Algeria) and DGRSDT (Direction Générale de la Recherche Scientifique et du développement Technologique, Algeria) for financial support.

CRediT author statement

Imen Sehout: Investigation; **Houssem Boulebd:** Theoretical calculations, Formal analysis, Writing – original draft, Visualization, Writing – review and editing; **Raouf Boulcina:** Writing – original draft**; Sara Nemouchi**: Investigation**; Amina Bramki**: Investigation; **Lamia Bendjeddou:** Investigation; **Hocine Merazig:** Resources; **Abdelmadjid Debache:** Conceptualization, Supervision.

Declaration of interests

The authors declare that they have no known competing financial interests or personal relationships that could have appeared to influence the work reported in this paper.

References

[1] R. Dua, S. Shrivastava, S.K. Sonwane, S.K. Srivastava, Pharmacological significance of synthetic heterocycles scaffold: a review, Advances in Biological Research 5(3) (2011) 120-144.
[2] K. Chand, A. Hiremathad, M. Singh, M.A. Santos, R.S. Keri, A review on antioxidant potential of bioactive heterocycle benzofuran: Natural and synthetic derivatives, Pharmacological Reports 69(2) (2017) 281-295.
[3] A.E. Goetz, T.K. Shah, N.K. Garg, Pyridynes and indolynes as building blocks for functionalized heterocycles and natural products, Chemical Communications 51(1) (2015) 34-45.
[4] V. Kumar, K. Kaur, G.K. Gupta, A.K. Sharma, Pyrazole containing natural products: synthetic preview and biological significance, European journal of medicinal chemistry 69 (2013) 735-753.
[5] M.F. Khan, M.M. Alam, G. Verma, W. Akhtar, M. Akhter, M. Shaquiquzzaman, The therapeutic voyage of pyrazole and its analogs: a review, European journal of medicinal chemistry 120 (2016) 170-201.
[6] K. Karrouchi, S. Radi, Y. Ramli, J. Taoufik, Y.N. Mabkhot, F.A. Al-aizari, Synthesis and pharmacological activities of pyrazole derivatives: a review, Molecules 23(1) (2018) 134.
[7] A. Chauhan, P.K. Sharma, N. Kaushik, Pyrazole: a versatile moiety, Int. J. ChemTech Res 3(1) (2011) 11-17.
[8] R. Mukherjee, Coordination chemistry with pyrazole-based chelating ligands: molecular structural aspects, Coordination Chemistry Reviews 203(1) (2000) 151-218.
[9] D.A. Horton, G.T. Bourne, M.L. Smythe, The combinatorial synthesis of bicyclic privileged structures or privileged substructures, Chemical reviews 103(3) (2003) 893-930.
[10] M. Verleye, I. Heulard, J.-M. Gillardin, Phenazone potentiates the local anaesthetic effect of lidocaine in mice, Pharmacological research 41(5) (2000) 539-542.
[11] F. Arellano, J.A. Sacristán, Metamizole: reassessment of its therapeutic role, European journal of clinical pharmacology 38(6) (1990) 617-619.
[12] H.G. Kraetsch, T. Hummel, J. Lötsch, R. Kussat, G. Kobal, Analgesic effects of propyphenazone in comparison to its combination with caffeine, European journal of clinical pharmacology 49(5) (1996) 377-382.
[13] A.G. Lipman, MARTINDALE: 'Martindale — the Extra Pharmacopoeia' (30th ed), edited by J. E. F. Reynolds, International Journal of Pharmacy Practice 2(2) (1993) 124-124.
[14] G. Mariappan, B.P. Saha, N.R. Bhuyan, P.R. Bharti, D. Kumar, Evaluation of antioxidant potential of pyrazolone derivatives, Journal of advanced pharmaceutical technology & research 1(2) (2010) 260.
[15] H.-J. Park, K. Lee, S.-J. Park, B. Ahn, J.-C. Lee, H. Cho, K.-I. Lee, Identification of antitumor activity of pyrazole oxime ethers, Bioorganic & medicinal chemistry letters 15(13) (2005) 3307-3312.
[16] Z. Xu, C. Gao, Q.-C. Ren, X.-F. Song, L.-S. Feng, Z.-S. Lv, Recent advances of pyrazole-containing derivatives as anti-tubercular agents, European journal of medicinal chemistry 139 (2017) 429-440.
[17] R. Thomas, Y.S. Mary, K.S. Resmi, B. Narayana, B.K. Sarojini, G. Vijayakumar, C. Van Alsenoy, Two neoteric pyrazole compounds as potential anti-cancer agents: Synthesis, electronic structure, physico-chemical properties and docking analysis, Journal of Molecular Structure 1181 (2019) 455-466.

[18] A.A. Bekhit, H.M.A. Ashour, A.A. Guemei, Novel Pyrazole Derivatives as Potential Promising Anti-inflammatory Antimicrobial Agents, Archiv der Pharmazie: An International Journal Pharmaceutical and Medicinal Chemistry 338(4) (2005) 167-174.
[19] G.H. Sayed, M.E. Azab, K.E. Anwer, M.A. Raouf, N.A. Negm, Pyrazole, pyrazolone and enaminonitrile pyrazole derivatives: Synthesis, characterization and potential in corrosion inhibition and antimicrobial applications, Journal of Molecular Liquids 252 (2018) 329-338.
[20] F. Marchetti, J. Palmucci, C. Pettinari, R. Pettinari, M. Marangoni, S. Ferraro, R. Giovannetti, S. Scuri, I. Grappasonni, M. Cocchioni, F.J. Maldonado Hodar, R. Gunnella, Preparation of Polyethylene Composites Containing Silver(I) Acylpyrazolonato Additives and SAR Investigation of their Antibacterial Activity, ACS Applied Materials & Interfaces 8(43) (2016) 29676-29687.
[21] S. Scuri, F. Petrelli, I. Grappasonni, L. Idemudia, F. Marchetti, C. Di Nicola, Evaluation of the antimicrobial activity of novel composite plastics containing two silver (I) additives, acyl pyrazolonate and acyl pyrazolone, Acta Bio Medica Atenei Parmensis 90(3) (2019) 370-377.
[22] F. Karcı, N. Ertan, Hetarylazo disperse dyes derived from 3-methyl-1-(3', 5'-dipiperidino-s-triazinyl)-5-pyrazolone as coupling component, Dyes and pigments 55(2-3) (2002) 99-108.
[23] F. Karcı, F. Karcı, Synthesis and absorption spectra of some novel heterocyclic disazo dyes derived from pyridone and pyrazolone derivatives, Dyes and pigments 76(1) (2008) 147-157.
[24] N.J. Parmar, H.A. Barad, B.R. Pansuriya, R.A. Patel, Chelation and extraction of copper (II) with 5-pyrazolone-based Schiff bases, Journal of Coordination Chemistry 64(4) (2011) 688-698.
[25] J.-W. Byun, D.-H. Lee, Y.-S. Lee, Preparation of polymer-bound pyrazolone active esters for combinatorial chemistry, Tetrahedron letters 44(44) (2003) 8063-8067.
[26] C. Leonelli, T.J. Mason, Microwave and ultrasonic processing: now a realistic option for industry, Chemical Engineering and Processing: Process Intensification 49(9) (2010) 885-900.
[27] B. Banerjee, Recent developments on ultrasound assisted catalyst-free organic synthesis, Ultrasonics sonochemistry 35 (2017) 1-14.
[28] A. Ziadi Chibane, R. Boulcina, H. Boulebd, C. Bensouici, M. Yildirim, A. Debache, Green one-pot multicomponent synthesis, biological evaluation and theoretical investigations of some novel β-acetamido ketone derivatives as potent cholinesterase inhibitors, Tetrahedron 76(25) (2020) 131260.
[29] K. Boudebbous, H. Boulebd, R. Boulcina, L. Bendjeddou, C. Bensouici, H. Merazig, A. Debache, Synthesis, crystal structure, biological evaluation, docking study, and DFT calculations of 1-amidoalkyl-2-naphthol derivative, Journal of Molecular Structure 1212 (2020) 128179.
[30] K. Boudebbous, H. Boulebd, C. Bensouici, D. Harakat, R. Boulcina, A. Debache, Synthesis, Docking Study and Biological Activities Evaluation of 1-Amidoalkyl-2-naphthol Derivatives as Dual Inhibitors of Cholinesterase and α-Glucosidase, ChemistrySelect 5(19) (2020) 5515-5520.
[31] M.I. Chouiter, H. Boulebd, D.M. Pereira, P. Valentão, P.B. Andrade, A. Belfaitah, A.M.S. Silva, New chalcone-type compounds and 2-pyrazoline derivatives: synthesis and caspase-dependent anticancer activity, Future Medicinal Chemistry 12(6) (2020) 493-509.
[32] C. Derabli, H. Boulebd, A.B. Abdelwahab, C. Boucheraine, S. Zerrouki, C. Bensouici, G. Kirsch, R. Boulcina, A. Debache, Synthesis, biological evaluation and molecular docking studies of novel 2-alkylthiopyrimidino-tacrines as anticholinesterase agents and their DFT calculations, Journal of Molecular Structure 1209 (2020) 127902.

[33] A. Altomare, G. Cascarano, C. Giacovazzo, A. Guagliardi, Completion and refinement of crystal structures with SIR92, Journal of Applied Crystallography 26(3) (1993) 343-350.
[34] G.M. Sheldrick, SHELXT–Integrated space-group and crystal-structure determination, Acta Crystallographica Section A: Foundations and Advances 71(1) (2015) 3-8.
[35] L.J. Farrugia, WinGX and ORTEP for Windows: an update, Journal of Applied Crystallography 45(4) (2012) 849-854.
[36] C.F. Macrae, P.R. Edgington, P. McCabe, E. Pidcock, G.P. Shields, R. Taylor, M. Towler, J.V.D. Streek, Mercury: visualization and analysis of crystal structures, Journal of Applied Crystallography 39(3) (2006) 453-457.
[37] M. J. Frisch, G. W. Trucks, H. B. Schlegel, G. E. Scuseria, M. A. Robb, J. R. Cheeseman, G. Scalmani, V. Barone, B. Mennucci, G. A. Petersson, H. Nakatsuji, M. Caricato, X. Li, A.F.I. H. P. Hratchian, J. Bloino, G. Zheng,, M.H. J. L. Sonnenberg, M. Ehara, K. Toyota,, J.H. R. Fukuda, M. Ishida, T. Nakajima, Y. Honda,, H.N. O. Kitao, T. Vreven, J. A. Montgomery Jr,, F.O. J. E. Peralta, M. J. Bearpark, J. Heyd,, K.N.K. E. N. Brothers, V. N. Staroverov, R. Kobayashi,, K.R. J. Normand, A. P. Rendell, J. C. Burant,, J.T. S. S. Iyengar, M. Cossi, N. Rega, N. J. Millam,, J.E.K. M. Klene, J. B. Cross, V. Bakken, C. Adamo,, R.G. J. Jaramillo, R. E. Stratmann, O. Yazyev,, R.C. A. J. Austin, C. Pomelli, J. W. Ochterski,, K.M. R. L. Martin, V. G. Zakrzewski, G. A. Voth,, J.J.D. P. Salvador, S. Dapprich, A. D. Daniels,, J.B.F. ¨ O. Farkas, J. V. Ortiz, J. Cioslowski,, D. J. Fox, Gaussian 09, Gaussian, Inc., Wallingford CT, (2009).
[38] A.D. Becke, Density-functional exchange-energy approximation with correct asymptotic behavior, Physical review A 38(6) (1988) 3098.
[39] P.C. Hariharan, J.A. Pople, The influence of polarization functions on molecular orbital hydrogenation energies, Theoretica chimica acta 28(3) (1973) 213-222.
[40] A. Benhassine, H. Boulebd, B. Anak, M.K. Ali, A. Bouraiou, H. Merazig, N. Kacem-Chaouche, A. Belfaitah, Co (II) complexes derived from (1-methyl-1H-imidazol-2-yl) methanol: Synthesis, characterization, spectroscopic study, DFT/TD-DFT calculations and biological evaluation, Inorganica Chimica Acta (2019) 119073.
[41] H. Boulebd, Y.D. Lahneche, I.A. Khodja, M. Benslimane, A. Belfaitah, New Schiff bases derived from benzimidazole as efficient mercury-complexing agents in aqueous medium, Journal of Molecular Structure 1196 (2019) 58-65.
[42] H. Boulebd, Comparative study of the radical scavenging behavior of ascorbic acid, BHT, BHA and Trolox: Experimental and theoretical study, Journal of Molecular Structure 1201 (2020) 127210.
[43] H. Boulebd, DFT study of the antiradical properties of some aromatic compounds derived from antioxidant essential oils: C–H bond vs. O–H bond, Free Radical Research 53(11-12) (2019) 1125-1134.
[44] H. Boulebd, I. Amine Khodja, M.V. Bay, N.T. Hoa, A. Mechler, Q.V. Vo, Thermodynamic and Kinetic Studies of the Radical Scavenging Behavior of Hydralazine and Dihydralazine: Theoretical Insights, The Journal of Physical Chemistry B 124(20) (2020) 4123-4131.
[45] H. Boulebd, The role of benzylic-allylic hydrogen atoms on the antiradical activity of prenylated natural chalcones: a thermodynamic and kinetic study, Journal of Biomolecular Structure and Dynamics (2020) 1-10.
[46] F.D. Gonelimali, J. Lin, W. Miao, J. Xuan, F. Charles, M. Chen, S.R. Hatab, Antimicrobial properties and mechanism of action of some plant extracts against food pathogens and spoilage microorganisms, Frontiers in microbiology 9 (2018) 1639.
[47] M. Yamaç, F. Bilgili, Antimicrobial activities of fruit bodies and/or mycelial cultures of some mushroom isolates, Pharmaceutical biology 44(9) (2006) 660-667.

[48] N.A.M.N. Hazalin, K. Ramasamy, S.S.M. Lim, I.A. Wahab, A.L.J. Cole, A.B.A. Majeed, Cytotoxic and antibacterial activities of endophytic fungi isolated from plants at the National Park, Pahang, Malaysia, BMC complementary and alternative medicine 9(1) (2009) 46.
[49] F.H. Allen, O. Kennard, D.G. Watson, L. Brammer, A.G. Orpen, R. Taylor, Tables of bond lengths determined by X-ray and neutron diffraction. Part 1. Bond lengths in organic compounds, Journal of the Chemical Society, Perkin Transactions 2 (12) (1987) S1-S19.
[50] J.L. Wardell, J.M.S. Skakle, J.N. Low, C. Glidewell, Cyclic and acyclic products from the reactions between methyl 3-oxobutanoate and arylhydrazines, Acta Crystallographica Section C: Crystal Structure Communications 63(8) (2007) o462-o467.
[51] C.C. He, G.C. Xu, Crystal structure of (Z)-N'-[1-(3-methyl-5-oxo-1-phenyl-1, 5-dihydro-4H-pyrazol-4-ylidene) propyl] benzenesulfonohydrazide, Acta Crystallographica Section E: Crystallographic Communications 71(5) (2015) 487-489.
[52] M.C. Etter, Encoding and decoding hydrogen-bond patterns of organic compounds, Accounts of Chemical Research 23(4) (1990) 120-126.
[53] M.J. Turner, J.J. McKinnon, S.K. Wolff, D.J. Grimwood, P.R. Spackman, D. Jayatilaka, M.A. Spackman, CrystalExplorer (Version 17.5), (2017).
[54] A. Nataraj, V. Balachandran, T. Karthick, Molecular structure, vibrational spectra, first hyperpolarizability and HOMO–LUMO analysis of p-acetylbenzonitrile using quantum chemical calculation, Journal of Molecular Structure 1038 (2013) 134-144.
[55] K.G. Krishnan, C.U. Kumar, W.-M. Lim, C.-W. Mai, P.V. Thanikachalam, C. Ramalingan, Novel cyanoacetamide integrated phenothiazines: Synthesis, characterization, computational studies and in vitro antioxidant and anticancer evaluations, Journal of Molecular Structure 1199 (2020) 127037.
[56] Y.-Y. Cai, L.-Y. Xu, L.-Q. Chai, Y.-X. Li, Synthesis, crystal structure, TD/DFT calculations and Hirshfeld surface analysis of 1-(4-((Benzo)dioxol-5-ylmethyleneamino)phenyl)ethanone oxime, Journal of Molecular Structure 1204 (2020) 127552.
[57] M. Kumar, M. Kariem, H.N. Sheikh, A. Frontera, S.K. Seth, A.K. Jassal, A series of 3D lanthanide coordination polymers decorated with a rigid 3,5-pyridinedicarboxylic acid linker: syntheses, structural diversity, DFT study, Hirshfeld surface analysis, luminescence and magnetic properties, Dalton Transactions 47(35) (2018) 12318-12336.
[58] İ. Sıdır, Y.G. Sıdır, M. Kumalar, E. Taşal, Ab initio Hartree–Fock and density functional theory investigations on the conformational stability, molecular structure and vibrational spectra of 7-acetoxy-6-(2,3-dibromopropyl)-4,8-dimethylcoumarin molecule, Journal of Molecular Structure 964(1) (2010) 134-151.
[59] K. Padmavathy, K.G. Krishnan, C.U. Kumar, P. Sutha, R. Sivaramakarthikeyan, C. Ramalingan, Synthesis, Antioxidant Evaluation, Density Functional Theory Study of Dihydropyrimidine Festooned Phenothiazines, ChemistrySelect 3(21) (2018) 5965-5974.
[60] P.K. Bayannavar, M.S. Sannaikar, S. Madan Kumar, S.R. Inamdar, S.K.J. Shaikh, A.R. Nesaragi, R.R. Kamble, Synthesis, X-ray characterization, DFT studies and Hirshfeld surface analysis of new organic single crystal: 2-(4-Methoxyphenyl)-4-{[2'-(1H-tetrazol-5-yl)biphenyl-4-yl] methyl}-2,4-dihydro-3H-1,2,4-triazol-3-one (MTBT), Journal of Molecular Structure 1179 (2019) 809-819.
[61] P.K. Chattaraj, U. Sarkar, D.R. Roy, Electrophilicity Index, Chemical Reviews 106(6) (2006) 2065-2091.
[62] R.G. Parr, L.v. Szentpály, S. Liu, Electrophilicity Index, Journal of the American Chemical Society 121(9) (1999) 1922-1924.

[63] R. Praveena, K. Sadasivam, V. Deepha, R. Sivakumar, Antioxidant potential of orientin: A combined experimental and DFT approach, Journal of Molecular Structure 1061 (2014) 114-123.
[64] C.G. Kumar, P. Mongolla, J. Joseph, Y.V.D. Nageswar, A. Kamal, Antimicrobial activity from the extracts of fungal isolates of soil and dung samples from Kaziranga National Park, Assam, India, Journal de Mycologie Médicale 20(4) (2010) 283-289.
[65] H.M. Atta, S.M. Dabour, S.G. Desoukey, Sparsomycin antibiotic production by Streptomyces sp. AZ-NIOFD1: taxonomy, fermentation, purification and biological activities, J. Agric. Environ. Sci 5 (2009) 368-377.
[66] P. Khloya, P. Kumar, A. Mittal, N.K. Aggarwal, P.K. Sharma, Synthesis of some novel 4-arylidene pyrazoles as potential antimicrobial agents, Organic and medicinal chemistry letters 3(1) (2013) 9.
[67] C.A. Lipinski, F. Lombardo, B.W. Dominy, P.J. Feeney, Experimental and computational approaches to estimate solubility and permeability in drug discovery and development settings, Advanced drug delivery reviews 23(1-3) (1997) 3-25.
[68] Y.H. Zhao, M.H. Abraham, J. Le, A. Hersey, C.N. Luscombe, G. Beck, B. Sherborne, I. Cooper, Rate-limited steps of human oral absorption and QSAR studies, Pharmaceutical research 19(10) (2002) 1446-1457.